Journal of Sound and Vibration (2003) **259**(4), 1000–1010
doi:10.1006/jsvi.2002.5376, available online at http://www.idealibrary.com on IDEAL®

FEATURE EXTRACTION OF THE RUB-IMPACT ROTOR SYSTEM BY MEANS OF WAVELET ANALYSIS

Z. Peng, Y. He, Q. Lu and F. Chu

Department of Precision Instruments, Tsinghua University, Beijing 100084*, People's Republic of China*
E-mail: Chufl@pim.tsinghua.edu.cn

(*Received* 12 *April* 2002, *and in final form* 21 *May* 2002)

1. INTRODUCTION

For rotating machines, the rub-impact between rotor and stator is a kind of serious malfunction, which often occurs at the positions with small clearances. This fault will bring a serious hazard to machines. For example, the rub impact between blades and seals will result in blade breakdown. The factors that influence rub-impact between rotor and stator are complicated, and the dynamic behavior of a rub impact rotor system is often non-linear. A comprehensive research has been performed based on the vibration information of a rub-impact rotor system. Muszynska's literature survey [1] gave a list of previous publications on the rub-related vibration phenomena during rubbing. Chu and Zhang [2] discussed periodic, quasi-periodic and chaotic vibrations of the rubbing system. Huang [3] studied the characteristics of the torsional vibration of a rotor with rub fault and found that the measured natural torsional frequency with rub is higher than the one without rub. Choy *et al.* [4] used the modal method to analyze the complex rotor-bearing-blade-casing system during component rub interactions. In Lin's paper [5], a simplified model is used to calculate the dynamic response of the rotor when it rubs with its housing, and some factors' effects are investigated. Smalley [6] studied the rub-induced thermal bow vibration during acceleration or deceleration of a steam turbine rotor. Based on these researches, some dynamic characteristics such as orbital presentation of shaft motion and the existence of strong higher harmonics can be used to judge whether a rotor system has rubbing or not. For all methods mentioned above, the Fourier transform has an important role in the analysis of the vibration signals of the rub-impact rotor system. It is well known, however, that the Fourier analysis has some inherent limitations in the analysis of the non-linear phenomena and it often cannot characterize the behaviors of rub-impact rotor system well.

Over the past 10 years, the wavelet theory [7] has become one of the emerging and fast-evolving mathematical and signal processing tools for its many distinct merits. Different from the fast-Fourier transform (FFT), the wavelet transform can be used for multi–scale analysis of the signal through dilation and translation, so it can extract the time-frequency features of the signals effectively. In the field of mechanical signal processing, wavelet transform has been used for noise purging [8] and feature extraction [9]. The present study specifically addresses the non-linear dynamic behaviors of the rub-impact rotor system and extracts the time–frequency features for fault diagnosis by means of the wavelet scalogram and the wavelet phase spectrum.

0022-460X/02/$35.00

2. CONTINUOUS WAVELET TRANSFORM

The driving force behind the wavelet transform is to overcome the disadvantages of the short-time Fourier transform (STFT), which provides constant resolution for all frequencies since it uses the same window for the analysis of the entire signal. The wavelet transform can achieve multi-resolution for it uses the different window functions for analyzing different frequency band of the signal $x(t)$. The window functions $\psi_{a,b}(t)$, which are named son wavelets, are all generated by dilation or compression of a prototype function $\psi(t)$, named the mother wavelet. The continuous wavelet transform of $x(t)$ is defined as follows:

$$W_x(a,b;\psi) = \langle x(t), \psi_{a,b}(t)\rangle = a^{-1/2}\int x(t)\psi^*_{a,b}(t)\,\mathrm{d}t, \quad a>0, \tag{1}$$

where

$$\psi_{a,b}(t) = a^{-1/2}\psi\left(\frac{t-b}{a}\right), \tag{2}$$

where a is the scale parameter, b is the time parameter, and both of them vary continuously. The factor $a^{-1/2}$ is used to ensure energy preservation for transform. The mother wavelet must satisfy the admissibility conditions, which require the mother function to be of finite support and of oscillatory.

The wavelet transform is a linear transform, whose physical pattern is to use a series of oscillating functions with different frequencies as window functions $\psi_{a,b}(t)$ to scan and translate the signal of $x(t)$, where a is the dilation parameter for changing the oscillating frequency. Although the wavelet transform is similar to the short Fourier transform in a certain sense, the difference between them exists. Compared with the short Fourier transform [10], whose time–frequency resolution is constant, the time–frequency resolution of the wavelet transform depends on the frequency of the signal. At high frequencies, the wavelet transform gives a high time resolution but a low frequency resolution. At low frequencies, high frequency resolution and low time resolution can be obtained.

The Morlet wavelet will be used throughout this paper. It is a kind of complex wavelet and can extract the amplitude and phase information of the signals. The Morlet wavelet is defined as follows:

$$\psi(t) = \pi^{-1/4}(\mathrm{e}^{-\mathrm{i}\omega_0 t} - \mathrm{e}^{-\omega_0^2/2})\mathrm{e}^{-t^2/2}. \tag{3}$$

Its Fourier transform is defined by

$$\hat{\psi}(\omega) = \pi^{-1/4}[\mathrm{e}^{-(\omega-\omega_0)^2/2} - \mathrm{e}^{-\omega_0^2/2}\mathrm{e}^{-\omega^2/2}]. \tag{4}$$

There is a great deal of wavelets that could be used. However, the Morlet wavelet is particularly attractive for the signal analysis. First, the Morlet wavelet function is an exponentially sinusoidal signal and the damped sinusoidal is the common response of many dynamical systems. Secondly, the Morlet wavelet has a single frequency. If a signal correlates highly with a scaled Morlet wavelet, then the frequency of the wavelet indicates the frequency of the signal analyzed.

3. WAVELET SCALOGRAM AND PHASE SPECTRUM

For all $\psi(t)$, $x(t) \in L^2(R)$, the inverse wavelet transform of $x(t)$ is defined as

$$x(t) = \frac{1}{C_\psi} \int \int a^{-2} W_x(a, b; \psi) \psi_{a,b}(t) \, \mathrm{d}a \, \mathrm{d}b. \tag{5}$$

It can be known from equation (6) that the wavelet transform does not lose any information, and the energy is preservative for the transform. Therefore, equation (7) is tenable

$$\langle x(t), x(t) \rangle = \int |x(t)|^2 d_t = \frac{1}{C_\psi} \int a^{-2} \, \mathrm{d}a \int |W_x(a, b; \psi)|^2 \, \mathrm{d}b. \tag{6}$$

The item $|W_x(a, b; \psi)|^2$ is defined as the wavelet scalogram [7]. The wavelet scalogram has been widely used for the analysis of non-stationary signal, and the scalogram can be seen as a spectrum with a constant relative bandwidth.

The wavelet phase spectrum [11] is defined as follows:

$$\varpi_x(a, b; \psi) = tg^{-1}\left(\frac{\mathrm{Im}[W_x(a, b; \psi)]}{\mathrm{Re}[W_x(a, b; \psi)]}\right). \tag{7}$$

3.1. CHARACTERISTICS OF WAVELET SCALOGRAM AND PHASE SPECTRUM

To illustrate the characteristics of the wavelet scalogram and the phase spectrum, three different signals will be considered. They are

$$sig_1(t) = \begin{cases} \sin(6\pi t), & 0 \leqslant t \leqslant 1 \quad \text{(s)}, \\ 2\sin(24\pi(t-1)^2), & 1 \leqslant t \leqslant 2 \quad \text{(s)}, \end{cases}$$

$$sig_2(t) = \sin(6\pi t) + \sin(24\pi(t+1)^2), \quad 0 \leqslant t \leqslant 1,$$

$sig_3(t)$: a white-noise signal.

Both Sig_1 and Sig_2 contain a single harmonic component with frequency $\omega = 3$ Hz and a linear frequency modulated component, but the lifespan of the two components is different for the two signals. Sig_3 is a white-noise signal. All the three signals are non-linear time-variant signals. Figures 1–3 show the dynamic behaviors of the three signals in the time domain and the frequency domain. For Sig_1 and Sig_2, the component with the frequency $\omega = 3$ Hz can be seen through the FFT spectrums, but it cannot be known whether the component exists during all the signal's lifespan or not. Moreover, the FFT spectrums cannot give any significant information about the linear frequency modulated component, that is, we cannot know whether Sig_1 and Sig_2 contain the linear frequency modulated component or not. For the white-noise signal Sig_3, its spectrum also shows the property of the white noise; we cannot know whether Sig_3 is a white-noise signal or not

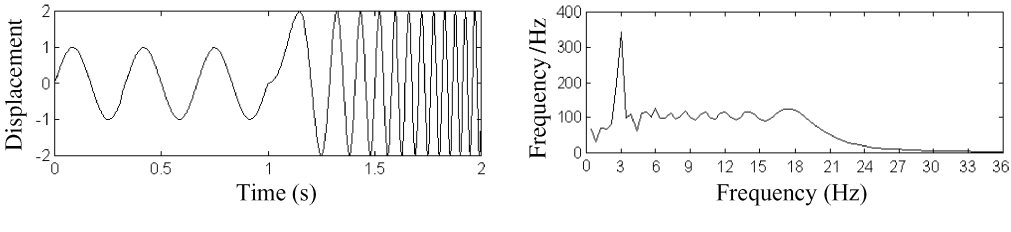

Figure 1. Test signal sig_1.

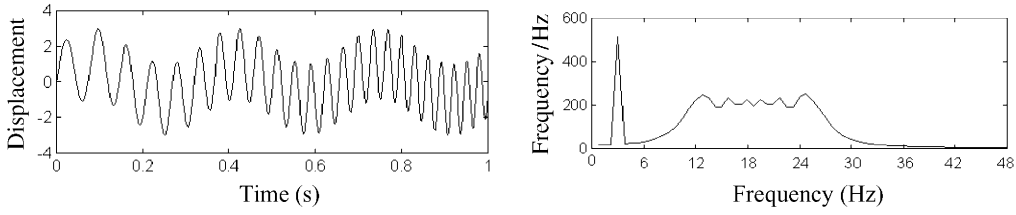

Figure 2. Test signal sig_2.

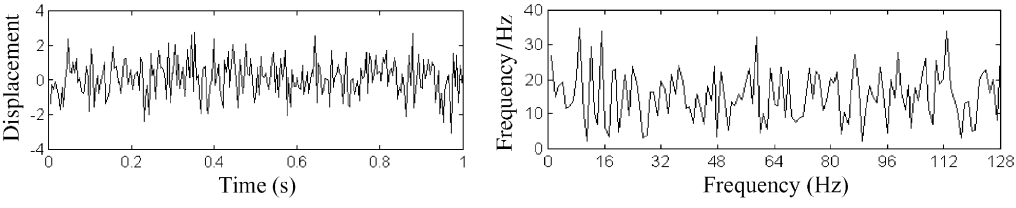

Figure 3. White-noise signal sig_3.

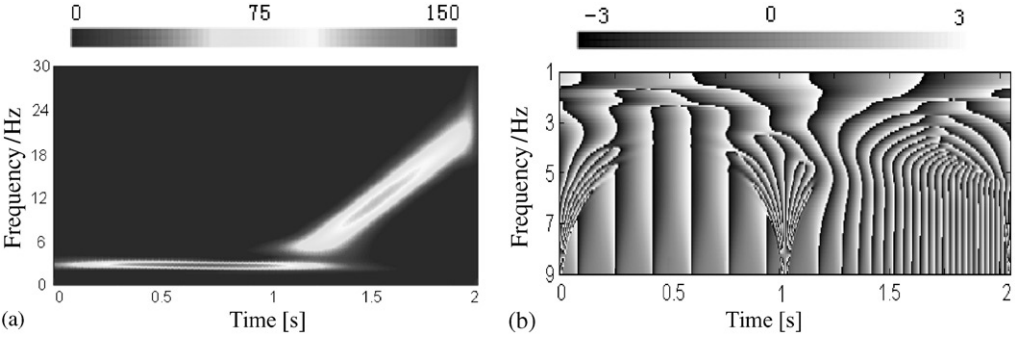

Figure 4. Scalogram and wavelet phase spectrum for the test signal sig_1: (a) scalogram; (b) wavelet phase spectrum.

just through the spectrum of the Sig_3. All the disadvantages of the FFT spectrum come from the integral transform utilized upon the signal globally. This transform smoothes the mutation component of the signal, and therefore the $\hat{f}(\omega)$ can only provide such spectral content with no indication about the time localization of the spectral components.

Figures 4(a), 5(a) and 6(a) are the wavelet scalograms of the three signals Sig_1, Sig_2 and Sig_3 respectively. In order to make a comparison with spectrums, a conversion from scale to central frequency is made. This conversion is reasonable because every wavelet is a band pass filter actually. The conversion can be expressed by

$$\omega = \omega_0/a, \tag{8}$$

where the ω_0 is the same as that in equation (4).

Obviously, the component with frequency $\omega = 3$ Hz and the linear frequency modulated component in the sig_1 and the sig_2 can be recognized through their scalograms. The two

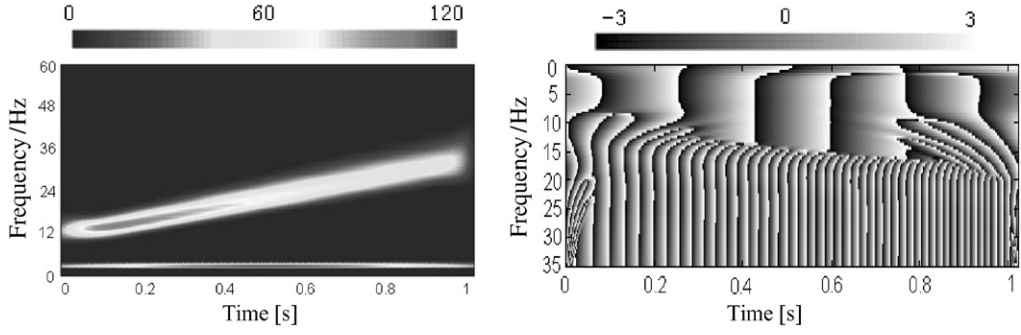

Figure 5. Scalogram and wavelet phase spectrum for the test signal sig_2: (a) scalogram; (b) wavelet phase spectrum.

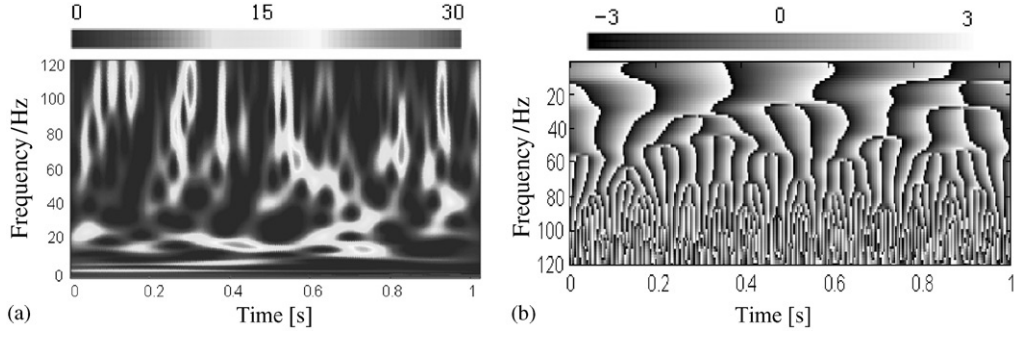

Figure 6. Scalogram and wavelet phase spectrum for the test signal sig_3: (a) scalogram; (b) wavelet phase spectrum.

components appear as a straight line segment and a skew line segment, respectively, on the scalograms. The straight line implies that the frequency of the component does not change with time and the skew line implies that the frequency of the component varies linearly with time, which is just the frequency feature of the linear frequency modulated signal. Moreover, the duration of each component can be known through the scalogram, for example, we can know that the duration of the linear frequency modulated component of sig_1 is about 1–2 *s* and that of sig_2 is 0–2 s. For sig_3, it is obvious that the white-noise signal has different frequencies at different time regions, and each frequency amplitude changes quickly with time (the value of the amplitude is expressed by color in the scalogram).

It can be seen that the concentration of the high frequency (small scale) is lower than that of the low frequency (big scale) in the scalogram, that is, the component with high frequency has wide bandwidth and the component with low frequency has narrow bandwidth. All of these are because the scalogram has a constant relative bandwidth. Therefore, the scalogram only has a limited resolution in the frequency domain, and when there exist two components with close frequencies in the same time, interference terms will emerge in the scalogram. Moreover, the time resolution at the low frequency is lower than that at high frequency in the scalogram. Due to those causes mentioned above, interference terms emerge in the region $1 < t < 1{\cdot}3$ s in the scalogram. It makes the component with the frequency $\omega = 3$ Hz, which should disappear from the scalogram at the time of $t = 1$ s, exist until the time $t = 1{\cdot}3$ s. Additionally, because the wavelet transform is performed on finite-length signals, border distortions arise [12]. The border distortion makes the amplitude at the boundary of the scalogram often smaller than that at the

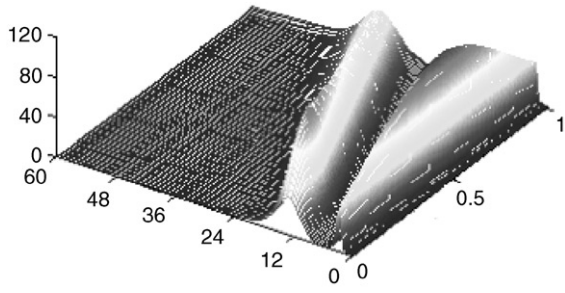

Figure 7. 3D graph of the signal sig_2 s scalogram.

middle of the scalogram. In order to better illustrate the impact of the border distortion on the scalogram, a 3D graph of the scalogram for sig_2 is given, as shown in Figure 7. It is obvious that the amplitudes of the component with frequency $\omega = 3$ Hz in the regions of 0–0·2 and 0·8–1 s are smaller than that in the region of 0·2–0·8 s. All these are the problems that we will encounter when using the scalogram to analyze signals, and we must deal with these problems carefully in practice.

Figures 4(b), 5(b) and 6(b) are the wavelet phase spectrums of the three signals sig_1, sig_2 and sig_3 respectively. For phase spectrums, the bandwidth denotes the signal period in the corresponding time region. At the frequency $\omega = 0$, the bandwidth is the length of the time region. As the frequency ω increases, the bandwidth keeps splitting to match the period of the signal until it fits the period of the signal. For example, the bandwidth of the sig_1's phase spectrum is constant during the time region of 0–1 s. It denotes that the frequency of the signal is constant during this time region; but the bandwidth narrows down gradually at the time region of 1–2 s, and this denotes that the frequency of the signal increases gradually at this time region. For the sig_2, it can be seen that the bands with constant bandwidth and the bands with narrowing down bandwidth co-exist at the whole time region, which denotes that there exist a component with constant frequency and a component with increasing frequency at the same time in the sig_2. For the sig_3s phase spectrum, the time when the bands split and the bandwidth are all uncertain, and this illustrates that the white-noise signal has different frequencies at different time. The analysis results obtained by the wavelet phase spectrum just accord with the results obtained by the scalogram.

In addition, it is obvious that there is a taper directing accurately to the frequency altering point (1 s) in the sig_1s phase spectrum. The taper is formed by the bands with constant phases. It is an inherent property for the wavelet phase spectrum no matter what the wavelet function chosen is, and therefore the phase spectrum can be used to localize the singular point. By the way, the border distortion will affect the wavelet phase spectrum as well. It is clearly visible in the phase spectrum of sig_1 and sig_2.

The analysis results above indicate that the wavelet scalogram and the wavelet phase spectrum have distinct advantages for the time-variant signal analysis. In the next section, the wavelet scalogram and the phase spectrum will be used to analyze the simulation signal and the experimental signal of the rub-impact fault in rotating machinery.

4. ANALYSIS AND DISCUSSION

The rub-impact is one of the malfunctions occurring often in the rotating machinery. The complexity of the rub-impact mechanism and the non-linearity of the rub-impact

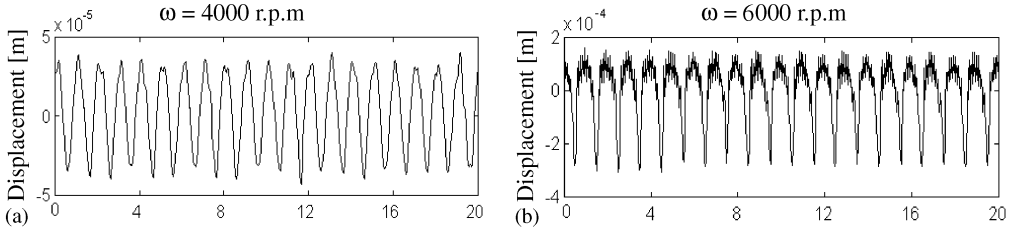

Figure 8. Simulation signals of the rub-impact fault (ordinates are in number of rotations): (a) signal of the slight rub-impact fault; (b) signal of the severe rub-impact fault.

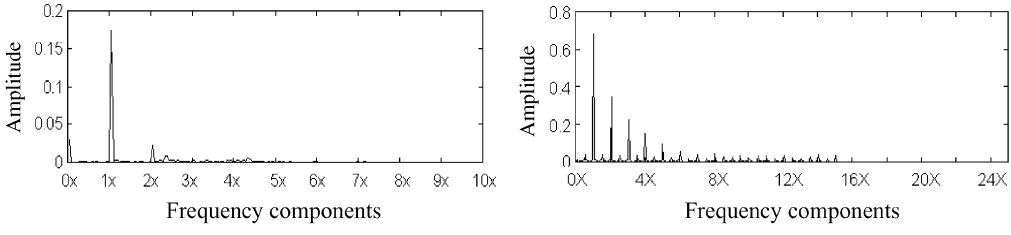

Figure 9. FFT spectrum of the rub-impact signal: (a) spectrum of the slight rub-impact fault; (b) spectrum of the severe rub-impact fault.

signals make it very difficult to analyze the behavior of the rub-impact rotor system and to extract the rub-impact fault features. Here, the scalogram and the wavelet phase spectrum are used to investigate the behavior of the rub-impact rotor and to extract the characteristic features.

4.1. NUMERICAL ANALYSIS FOR A RUB-IMPACT ROTOR

The simulation signals are obtained through the multi-disk rub-impact rotor model of reference [13]. Figures 8(a) and 8(b) show the dynamic behaviors of two sets of signals for the rub-impact fault in the time domain, which are obtained under different rotating speeds. At the rotating speed $\omega = 4000$ r.p.m, the slight rub-impact occurs, and at the rotating speed $\omega = 6000$ r.p.m, the severe rub-impact occurs. Their spectrums are shown as Figures 9(a) and 9(b) respectively. It can be seen that the slight rub impact has excited the components of $1X$, $2X$, etc. and the severe rub impact has excited the components of $1/2X$, $1X$, $3/2X$, $2X$, $3X$, etc, all these are just the frequency features of the rub impact fault. However, only through the FFT spectrum, we cannot know whether those components exist during the whole time region or they are just excited intermittently, and we cannot know whether the existing forms of those components are related to the degree of rub-impact fault or not. On the contrary, we can obtain all these information through the wavelet scalogram and the wavelet phase spectrum.

Figures 10(a) and 10(b) show the scalograms of the two sets of simulation signals of the rub-impact fault. Through the scalogram, it can be seen that when the slight rub impact occurs, the component of $1X$ exists during all the time and its amplitude changes only slightly; but the component of $2X$ is excited intermittently and its amplitude changes also slightly at each time of its appearance. For the components with higher frequencies, such

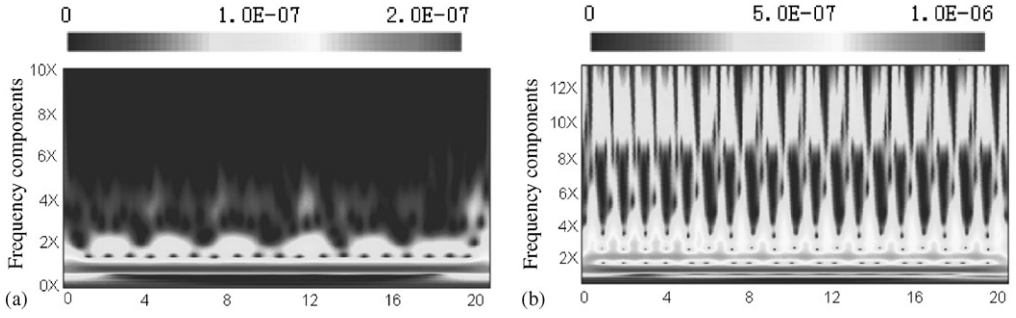

Figure 10. Scalogram of the rub-impact signals (ordinates are in number of rotations): (a) scalogram of the slight rub-impact fault; (b) scalogram of the severe rub-impact fault.

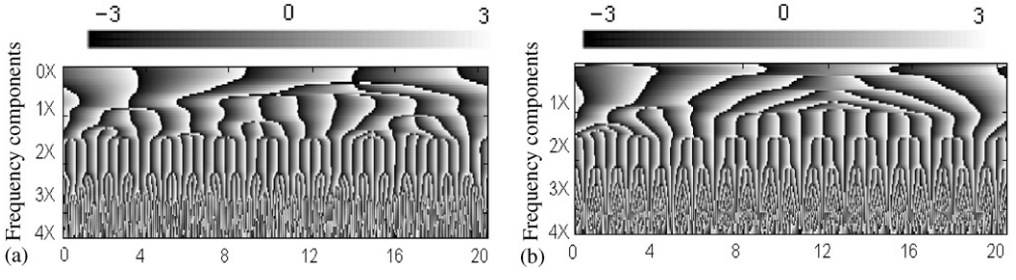

Figure 11. Phase spectrums of the rub-impact signals (ordinates are in number of rotations): (a) phase of the slight rub-impact fault; (b) phase of the severe rub-impact fault.

as the component of $4X$, they appear irregularly and their amplitudes are relatively lower. For the signals of the severe rub-impact fault, it is obvious that the components of $1X$, $2X$ exist during the whole time period and their amplitude changes only slightly. The components of $3X$, $4X$ exist during all the time as well, but their amplitudes change regularly with time. However, for the components with higher frequencies, such as the components of $5X$, $6X$, they are excited periodically in general and their amplitudes change slightly. Through the above analysis, the following conclusions can be obtained. The existing forms of the components of the rub-impact signals are relative to the degree of the rub-impact fault: in general, when the slight rub-impact occurs, only the components with low frequencies can exist during all the time in the scalogram, but the components with high frequencies will be excited intermittently; and when the severe rub-impact occurs, more components can exist continually, and the other components with higher frequencies are excited intermittently as well.

Figures 11(a) and 11(b) show the wavelet phase spectrums of the two sets of simulation signals for the rub-impact rotor. It can be seen that the phase spectrums look like that of the white-noise signal at the area of frequency $\omega > 3X$ where the bands split almost irregularly no matter what the degree of the rub-impact is. This reflects the complexity of the rub-impact signals.

4.2. EXPERIMENTAL RESULTS

In this section, the scalogram and the wavelet phase spectrum are used to analyze the experimental data of the rub-impact rotor. Figure 12 shows the experimental test rig,

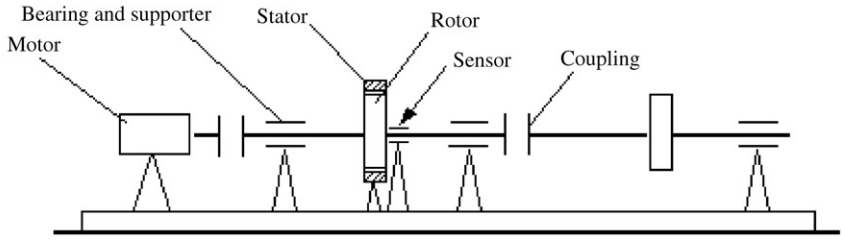

Figure 12. Experimental test rig.

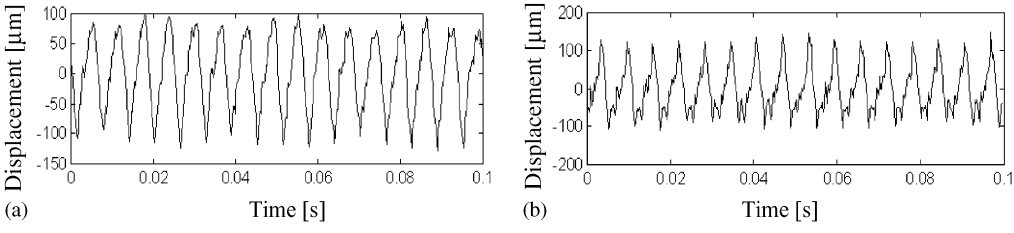

Figure 13. Experimental signals of the rub-impact fault: (a) signal of the slight rub-impact fault; (b) signal of the severe rub-impact fault.

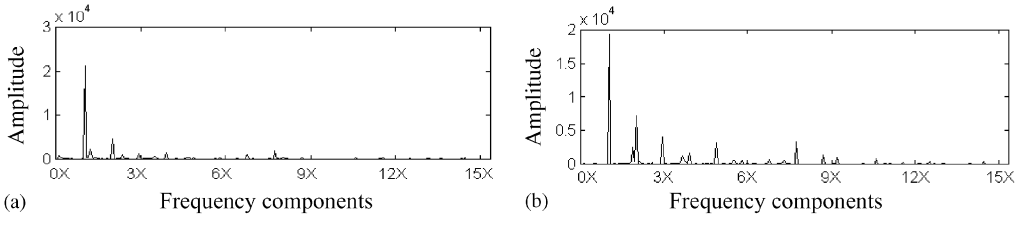

Figure 14. FFT spectrums of the rub-impact signals: (a) spectrum of the slight rub-impact fault; (b) spectrum of the severe rub-impact fault.

which is mainly composed of the rotor, a driving motor, journal bearings and couplings. Both vertical and horizontal vibration signals were picked up by non-contact eddy current transducers.

Reducing the clearance between the stator and the rotor will cause the radial rub. In order to create the rub with different severity, several stators with different diameters are prepared. To create the slight rub, the stator with big inner diameter is used, and to create the severe rub, the stator with small diameter is used. Figures 13(a) and 13(b) show two sets of horizontal vibration data that were sampled at a speed of 1·6 kHz. One set data was sampled under the slight rub-impact condition and the other set under the relatively severe rub-impact condition. The rotating speed is 3000 r/min. Their FFT spectrums are shown in Figures 14(a) and 14(b) respectively. Obviously, all the spectrums show the frequency features of the rub-impact fault.

Figures 15(a) and 15(b) show the scalograms of the two sets of experimental data. For Figure 15(a), it can be seen that the components of $1X$ and $2X$ exist at all time, but the amplitude of the component of $2X$ changes slightly. The other components with higher frequencies, such as the components of $4X$ and $7X$, appear only intermittently. All these features of the scalogram are the same as that of the scalogram with the slight rub impact,

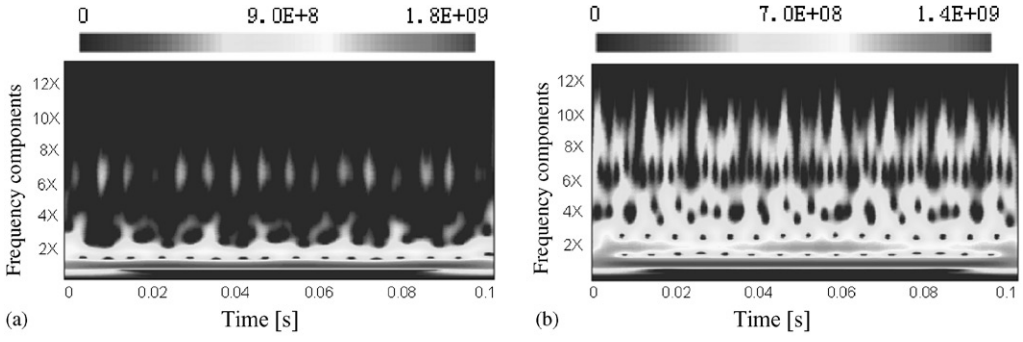

Figure 15. Scalograms of the rub-impact fault: (a) scalogram of the slight rub-impact fault; (b) scalogram of the severe rub-impact fault.

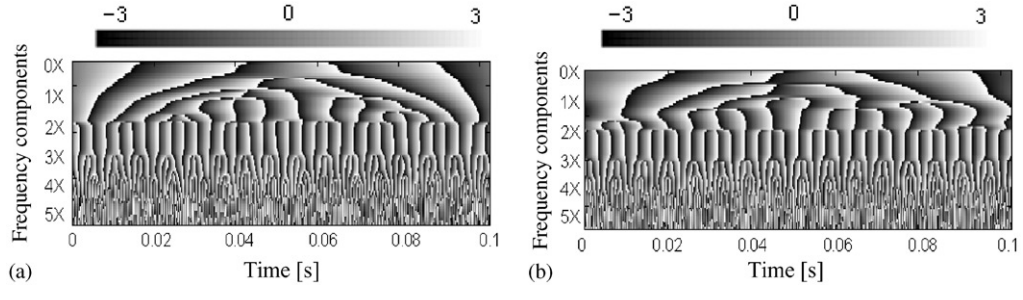

Figure 16. Phase spectrums of the rub-impact fault: (a) phase of the slight rub-impact fault; (b) phase of the severe rub-impact fault.

and therefore we can conclude that the slight rub impact occurs in the rotor system. For Figure 15(b), the component of $1X$ exists during the whole time period and its amplitude is constant; the components of $2X$ and $3X$ exist during all the time as well, but their amplitudes change regularly with time, and the change range is very small; the other components with higher frequencies, such as the components of $5X$ and $8X$, are excited only intermittently and their amplitudes change with time. All these characteristics are most likely to those of the severe rub-impact signals' scalogram and therefore we can conclude that there exists a severe rub impact in the rotor system.

Figures 16(a) and 16(b) show the wavelet phase spectrums of the two sets of experimental signals for the rub-impact rotor. Obviously, irregular splits occur in the area of frequency $\omega > 3X$ in both the wavelet phase spectrums, which are just the phase features of the rub impact.

It can be concluded that the scalogram and the wavelet phase spectrum have distinct advantages for the rub-impact signal analysis; and they can characterize the dynamical behavior of the rub-impact rotor better and can extract the rub-impact features well.

5. CONCLUSIONS

In this paper, three simulation signals are used to illustrate the characteristics of the scalogram and the wavelet phase spectrum, and the results indicate that the scalogram and the wavelet phase spectrum are very suitable to non-stationary signal analysis. Some problems about using the scalogram and the wavelet phase spectrum are discussed. Then

the scalogram and the wavelet phase spectrum are introduced to the analysis of the dynamical behaviors of the rotor system with rub-impact fault. Numerical and experimental examples are given, and the results show that the scalogram and the wavelet phase spectrum have distinct advantages for the rub-impact signal analysis compared with the FFT spectrum. Some new features of the rub impact are obtained as follows:

(1) When the slight rub impact occurs, only some components with low frequency can exist continually, while the other components with higher frequencies are excited intermittently and their amplitudes are small in general.
(2) When the severe rub impact occurs, besides some components with low frequency, there are more components that can exist continually, and some of their amplitudes will change slightly with regularity, but the other components with higher frequencies are still excited intermittently.
(3) When the rub-impact occurs, no matter slightly or severely, the bands will split almost irregularly in the area of frequency $\omega > 3X$ in the wavelet phase spectrum.

ACKNOWLEDGMENTS

This research is supported financially by National Natural Science Foundation of China (Grant No. 19990510).

REFERENCES

1. A. Muszynska 1989 *Shock and Vibration Digest* **21**, 3–11. Rotor-to-stationary element rub-related vibration phenomena in rotating machinery—literature survey.
2. F. Chu and Z. Zhang 1998 *Journal of Sound and Vibration* **210**, 1–18. Bifurcation and chaos in a rub-impact Jeffcott rotor system.
3. D. Huang 2000 *Tribology International* **33**, 75–79. Experiment on the characteristics of torsional vibration of rotor-to-stator rub in turbomachinery.
4. F. K. Choy, J. Padovan and C. Batur 1989 *Journal of Engineering for Gas Turbines and Power, Transactions of the American Society of Mechanical Engineers* **111**, 652–658. Rub interactions of flexible casing rotor systems.
5. F. Lin, M. P. Schoen and U. A. Korde 2001 *Journal of Vibration and Control* **7**, 833–848. Numerical investigation with rub-related vibration in rotating machinery.
6. A. J. Smalley 1989 *Journal of Vibration, Acoustics, Stress, and Reliability in Design* **111**, 226–233. Dynamic response of rotors to rubs during startup.
7. Z. Peng, F. Chu and Y. He. 2002 *Journal of Sound and Vibration* **253**, 1087–1100. Vibration signal analysis and feature extraction based on reassigned wavelet scalogram (to print).
8. N. Tandon and A. Choudhury 1999 *Tribology International* **32**, 469–480. Review of vibration and acoustic measurement methods for the detection of defects in rolling element bearings.
9. J. Lin and L. Qu 2000 *Journal of Sound and Vibration* **234**, 135–148. Feature extraction based on Morlet wavelet and its application for mechanical fault diagnosis.
10. P. C. Russell, J. Cosgrave, D. Tomtsis, A. Vourdas *et al.* 1998 *Measurement Science and Technology* **9**, 1282–1290. Extraction of information from acoustic vibration signals using Gabor transform type devices.
11. Lai Ah Wong and Jay Chung Chen 2001 *International Journal of Non-Linear Mechanics* **36**, 221–235. Nonlinear and chaotic behavior of structural system investigated by wavelet transform techniques.
12. J. X. Wei, M. R. Pickering, M. R. Frater and J. F. Arnold 2000 *Proceedings of SPIE* 4067, 1290–1295. New method for reducing boundary artifacts in block-based wavelet image compression.
13. F. Chu and W. Lu 2001 *Journal of Sound and Vibration* **248**, 235–246. Determination of the rubbing location in a multi-disk rotor system by means of dynamic stiffness identification.